Mechanical Behaviour of Air-plasma Sprayed Functionally Graded YSZ-Mullite Environmental Barrier Coatings: A Study via Instrumented Indentation

C. V. Cojocaru, Y. Wang, R. S. Lima, Boucherville/CND, C. Moreau, Montreal/CND, J. Mesquita-Guimarães, E. Garcia, P. Miranzo and M. I. Osendi, Madrid/E

Mullite ($Al_6Si_2O_{13}$) is the basis of efficient environmental barrier coatings (EBCs) for protecting Si-based ceramic matrix composites (CMCs) selected to replace specific hot-section metallic components in advanced gas turbines. Furthermore, YSZ-mullite multilayer architectures with compositional grading between the bond coat and YSZ top coat were envisioned as solutions to ease their coefficient of thermal expansion (CTE) mismatch induced stress. Consequently, a proper understanding of the mechanical properties such as the elastic modulus, hardness or plastic/elastic recovery work serve for an efficient design of such refractory oxide multilayers. In this work, three different mullite powder morphologies (fused and crushed, spray-dried and freeze-granulated) were employed. Using depth-sensing indentation with loads in the range 100 – 500 mN, the role of the microstructure and morphology of the powder feedstock on the mechanical behaviour of air plasma sprayed mullite bond coats deposited on SiC Hexoloy substrates was investigated. Fully crystalline as-sprayed mullite coatings were engineered under controlled deposition conditions. Mechanical properties were measured for the as-sprayed coatings as well as for coatings heat-treated at 1300°C, in water vapour environment, for periods up to 500 h. Both E and H values of the coatings are found to be highly dependent on the morphology of the starting powders.

1 Introduction

Environmental barrier coatings (EBCs) are multilayered coatings conceived and proposed to protect Si-based ceramics (e.g., SiC and Si_3N_4) in the quest to replace metallic components for instance in specific hot-sections of gas turbine engines [1]. Mullite ($Al_6Si_2O_{13}$) is a low cost refractory oxide that curently represents the building-block of an efficient environmental barrier coating architecture. Mullite has a low thermal expansion coefficient (4.5-5.6 x 10^{-6}/°C) that represents for instance a close match with SiC (4.02 x 10^{-6}/°C) and excellent high temperature properties (e.g., high thermal shock and thermal stress resistance) offered mainly by its interlocking grain structure [2] In addition to the above mentioned high-temperature properties, a second essential requirement of an EBC system is its stability in high temperature environments containing water vapours. A low permeability for oxidant species, good chemical compatibility with the Si-based substrate and silica scale formed from oxidation are mandatory features for an EBC so as to inhibit its major degradation mechanism namely the formation of volatile silicon hydroxide ($Si(OH)_4(g)$) when subjected to a corrosive water vapour containing environment originating from the combustion of the fuel (e.g., kerosene). Therefore, a suitable protective coating for gas turbine engine components formed of Si-containing materials essentially must fulfill a dual role serving as a thermal barrier and simultaneously providing environmental protection [3]. Mullite alone does not meet both requirements since it does not possess a good resistance to H_2O vapour attack [4] and a way to overcome this shortcoming is the usage of layered coatings that as an ensemble offers the sought functionality. Consequently, functionally graded materials, with discrete or continuous variations in composition and structure, showing corresponding changes in their properties have been introduced to applications where a certain functional requirement of a component is position dependent [5-6]. Mullite-based multilayer architectures for instance, with compositional grading between the mullite bond coat and a yttria stabilized zirconia (YSZ) top coat (showing excellent resistance to H_2O vapours attack) might offer a solution to ease their coefficient of thermal expansion (CTE) mismatch induced stress [7]. A proper understanding of the mechanical properties such as the elastic modulus, hardness or plastic/elastic recovery work serves for an efficient design of such refractory oxide multilayers.

In this work, three different mullite powder morphologies (fused and crushed, spray-dried and freeze-granulated) were employed. Using depth-sensing indentation with loads in the range 100 – 500 mN, the role of the microstructure and morphology of the powder feedstock on the mechanical behaviour of air plasma sprayed mullite bond coats deposited on SiC Hexaloy substrates was assesed. Fully crystalline as-sprayed mullite coatings were engineered under controlled deposition conditions. Their mechanical properties were measured for the as-sprayed coatings as well as for coatings heat-treated at 1300°C, in H_2O vapour environment, for periods up to 500 h. It was aimed the fabrication of an efficient and cost-effective EBC prototype based on YSZ compositionally graded mullite.

2 Experimental

2.1 Sample preparation

Three types of mullite powders with different morphologies and size distribution were employed in these studies: (i) fused and crushed (SG1020, Saint-Gobain, Worchester, MA, USA), (ii) spray-dried (further referred as M_30SD) and (iii) freeze-granulated (further referred as M_50FG) from Instituto de Ceramica y Vidrio (ICV) – CSIC, Madrid, Spain [8]. Scanning electron microscope (SEM) images and

particle size distribution of the mullite powders used are shown in **Fig.1.(a)-(c)**.

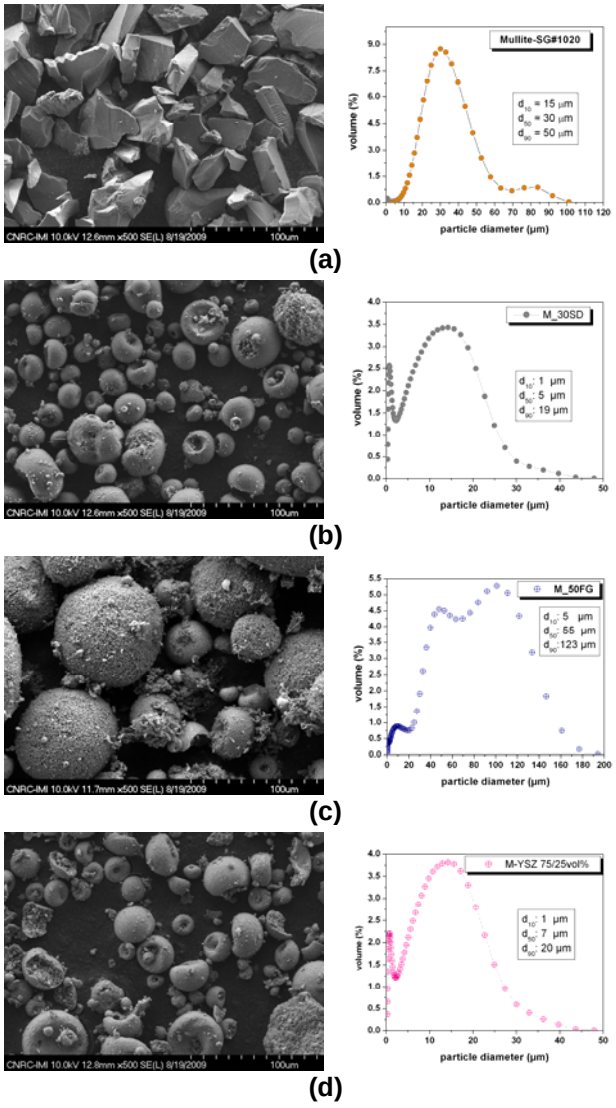

Fig. 1. SEM micrographs of the mullite powders used throughout the experiments and their corresponding size distribution.

The particle size distributions were measured using a laser scattering particle size analyser (LS 13320, Beckman Coulter, Miami, FL, USA). The morphology and size distribution of a mixed mullite-YSZ powder (75/25 vol.%) from ICV_CSIC, Madrid, Spain is also shown in **Fig.1.(d).** These mixtures were produced using as base-line the M_30SD mullite powders.

The powders were sprayed on SiC Hexoloy SA (Saint-Gobain, Worchester, MA, USA) 5 x 5 cm substrates, via atmospheric plasma spray (APS) technique (Axial III, Northwest Mettech, North Vancouver, BC, Canada). Fully crystalline as-deposited bond-coatings were engineered in all cases by employing a proprietary NRC technology [9]. Combinations of mullite/YSZ powders (ICV-CSIC Madrid, Spain) such as mullite-YSZ 75/25vol% and mullite-YSZ 50/50vol% have been further deposited on top of the mullite bond coats so as to produce bi and tri-layer coatings with a YSZ compositional grading.

After completing the spraying process the 5 x 5 cm coupons were cut in quarters for structural/mechanical analysis and thermal treatment (TT).

2.2 Structural characterization and thermal treatment

A diffractometer (D8-Discovery, Brucker AXS Inc. Madison, WI, USA) using Cu-Kα radiation in Bragg-Brentano (θ-2θ) configuration was used to analyze the phase composition of both as-prayed and thermally treated coatings. The diffracted signal was collected over a two-theta range of 20°-60° with a step size of 0.02° and a 5 sec/step acquisition time through a 1° fine collimator slit.

After XRD characterization, samples were embedded in epoxy prior to cross-section cutting and further prepared by standard metallographic procedures for field-emission scanning electron microscopy (FE-SEM) (S4700, Hitachi Ltd., Tokyo, Japan) and instrumented indentation testing (IIT) (Nanoindenter G200, Agilent Technologies, Oak Ridge, TN, USA).

Thermal treatment tests were performed at 1300°C, in a H_2O vapour environment (90%H_2O/10%air), for time intervals up to 500 h using an in-house developed EBC rig and based on a high-temperature tube furnace (STT-1700-2.0-18, SentroTech, Berea, OH, USA).

2.3 Mechanical testing via instrumented indentation testing (IIT)

Elastic modulus (E) and hardness (H) of each deposited coating were measured at room temperature on the polished cross-section of the sample, via Oliver-Pharr method (depth-sensing indentation) [10] making use of a Berkovich diamond tip. The applied indentation loads and the corresponding penetration depths (tip displacements into surface) are measured continuously during an loading-unloading cycle. Thus the main advantage of using depth-sensing indentation consists in the fact that the residual hardness impression does not have to be directly imaged as in conventional microhardness testing.

Hardness is calculated directly (in GPa) based on the formula:

$$H = \frac{P}{A}$$

where *P* is the load applied to the test surface and *A* is the projected contact area at that load.

The Young's modulus of the coating material is calculated based on the initial portion of the unloading

curve as the unloading is the purely elastic recovery process. This gives the elastic stiffness of the contact S and serves to initially determine the reduced elastic modulus (E_r):

$$S = \frac{dP}{dh} = 2\beta \frac{\sqrt{A}}{\sqrt{\pi}} E_r$$

E of the test material is calculated from E_r using:

$$\frac{1}{E_r} = \frac{1 - \nu^2}{E} + \frac{1 - \nu_i^2}{E_i}$$

The indenter diamond tip properties used for calculations are E_i=1141 GPa and Poisson's ratio ν_i=0.07 and a numerical factor β=1 for the triangular cross-sections like the Berkovich tip.

The measurements were performed at loads between 100-500 mN with loading times of 15 s and unloading (90% record of the segment) of 20 s. For each sample, sets of 15-20 indents were performed with distances between indents in the range of 25-50 microns and correlated with the applied load. Examples of indentation impressions onto the surfaces of the coatings are shown in **Fig. 2.**

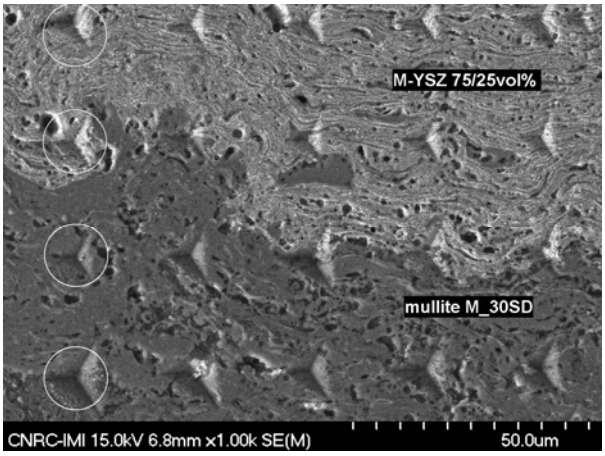

Fig. 2. Indentation testing residual impression arrays made into a mullite/mullite-YSZ75/25vol% by-layer with a Berkovich diamond tip.

Young's modulus was determined using the stiffness as calculated from the slope of the load-displacement curve during each unloading cycle. In these studies, the Poisson ratio's was assumed to be 0.25.

3 Results and discussion

3.1 Microstructural analysis

X-ray diffraction patterns revealed fully crystalline as-sprayed coatings in all cases (examples shown in **Fig. 3.**). The intrinsic nature and difference in the size distribution between the M_30SD (spray-dried) and SG (fused and crushed) mullite powders may explain the formation of a γ-Al_2O_3-rich phase observed within the M_30SD coatings.

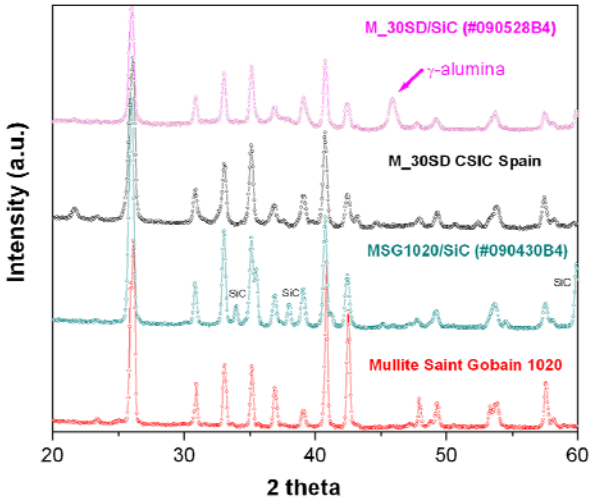

Fig. 3. XRD of mullite APS coatings.

Thermally treated coatings up to 500 h at 1300°C in H_2O vapour environment also exhibit a high degree of crystallinity. A detailed structural characterization of the coatings obtained is given elsewhere [11]. Typical as-sprayed bi-layer coating architectures obtained are shown in **Fig.4 (a)** and **(b).**

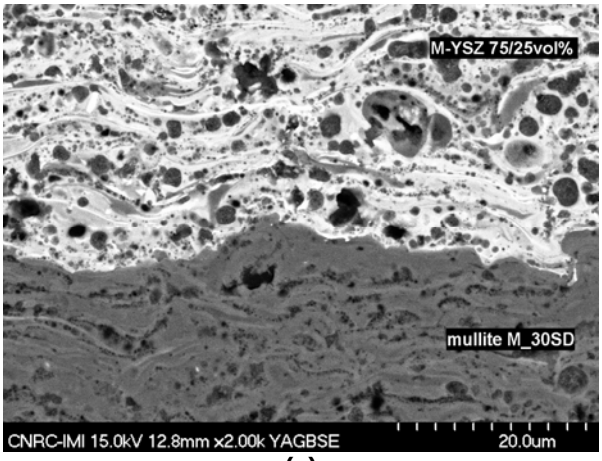

(a)

Fig. 4(a). SEM image of the as-sprayed mullite M_30SD/M-YSZ 75/25 vol% bi-layer.

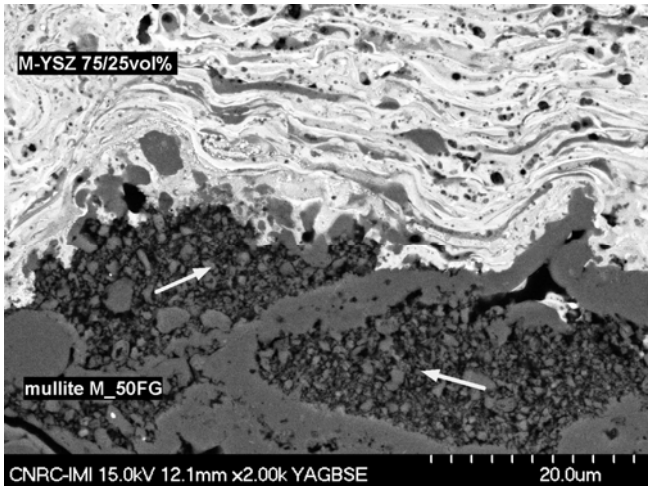

(b)

Fig. 4(b). SEM image of the as-sprayed mullite M_50FG/M-YSZ 75/25% bi-layers

The M_30SD powder based coatings appear to be the denser ones while the M_50FG powder based ones are exhibiting a higher amount of semi-molten (freeze-granulated) particles indicated by arrows in **Fig. 4 (b)**.

3.2 Indentation load effect

The influence of indentation load on both hardness and Young's modulus of ceramics has been investigated by several groups and it was reported that both H and E exhibit significant dependence on the indentation load [12]. The load on the sample is defined as the force with which the indenter tip is impinging on the surface and depth is measured from the contact point of the tip with the sample. A general trend is that hardness and elastic moduli tend to decrease with the increase of the load applied [13]. To verify these assumptions measurements were performed on the deposited coatings by varying the indentation loads from 10 to 500 mN and searching for the interval values of the applied force for which the H and E data obtained stabilized. A more detailed analysis on the indentation size effects on H and E values of plasma sprayed coatings is presented elsewhere [14]. Within the load interval 250-500 mN, both H and E values start to stabilize and at this point it is hypothesized that the measured values represent a global perspective on the material and not only probing small volumes of its microstructure.

3.3 Analysis of load-displacement curves

In the following the results of mechanical testing, obtained with an indentation load of 500 mN, on all the as-sprayed mullite layers is discussed.

Typical load-displacement curves recorded during indentation for all three types of mullite layers are depicted in **Fig. 5.** The load-depth curves during unloading reveal different slopes which means different Young's moduli.

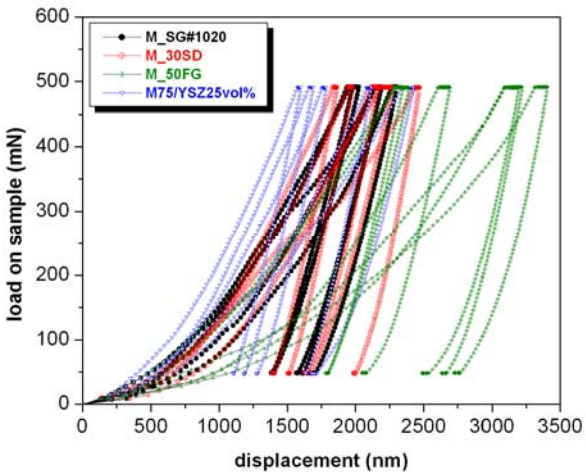

Fig. 5. Load-displacement indentation curves recorded in the as-sprayed coatings for an applied load of 500 mN.

Mean values (15 indentations) obtained for E and H for layered coating architectures both the as-sprayed state and thermally treated are provided in ***Table 1***.

Table 1. *E and H values of the as-sprayed and heat-treated coatings for time intervals up to 500 h (the green and yellow rows represent two bi-layer systems).*

coating	*As dep.* E[GPa] Std.dev	*As dep.* H[GPa] Std.dev	after *100h TT* E[GPa] Std.dev	after *100h* H[GPa] Std.dev	after *500h TT* E[GPa] Std.dev	after *500h TT* H[GPa] Std.dev
M_SG	96 ± 7	6.6 ± 1	99 ± 12	9.2 ± 1	161 ± 6	12 ± 2
M_30SD	118 ± 17	6.1 ± 2	155 ± 16	9.5 ± 2	172 ± 16	10 ± 2
M75/YSZ 25 vol%	127 ± 29	7.8 ± 3	139 ± 16	8.4 ± 2	168 ± 17	9.2 ± 1
M_50FG	90 ± 19	4.7 ± 2	69 ± 8	2.6 ± 1	69 ± 11	2.9 ± 1
M75/YSZ 25 vol%	156 ± 13	11.9 ± 2	162 ± 7	12.2 ± 2	157± 16	11.8 ± 2

By looking at ***Table 1*** it is observed that elastic modulus values for the mullite bond coats obtained with the fused and crushed M_SG powder are found to be smaller than the E values obtained for the coatings deposited with the custom prepared M_30SD. However, the coatings obtained with the M_50FG powder exhibit even smaller E and also H values when compared with the latter.

This result is in concordance with the densities and microstructures of the respective coatings that are dictated by the particle size distribution of the powders. The larger size distribution of the SG and M_50FG mullite powders will tend to generate higher porosity levels, which leads to a decrease in the hardness and elastic modulus values of the coatings. In addition, the M_50FG based coatings (**Fig. 4(b)**) appear to have a higher level of unmolten particles than the M_SG based coatings (not shown).

The effect of the thermal treatment on the elastic modulus and hardness of the deposited coatings was also investigated. The E and H values increase with the period time of the heat treatment and follow the general trend observed in ceramics (and basically in other materials).

Representative load-displacement curves of M_30SD bond-coatings that are part of a M-YSZ 75/25%vol / M_30SD/SiC architecture are shown in **Fig.6(a)** whereas in **Fig.6(b)** are shown similar curves recorded this time from a M-YSZ(75/25)vol.% M_50FG/SiC architecture.

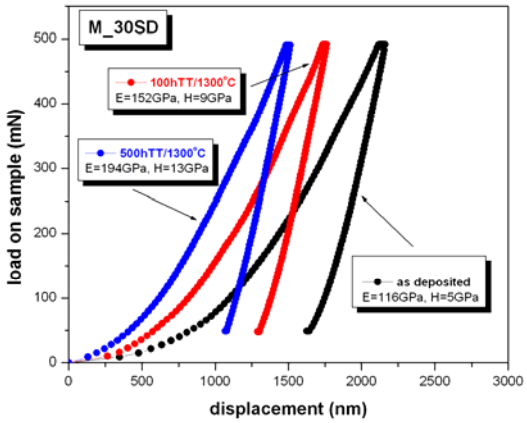

(a)

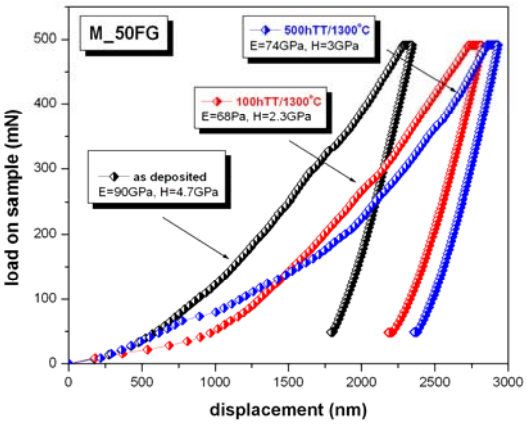

(b)

Fig.6. Load-displacement indentation curves recorded from as sprayed and thermally treated **(a)** M_30SD and **(b)** M_50FG mullite coatings for time intervals up to 500 h.

The values presented in ***Table 1*** suggest a better match between the E and H values of the M_30SD based bond coat and M75YSZ25 based layer than those between the M_50FG and M75/YSZ25 coatings.

It is hypothesized that a desirable layered architecture will be the one that demonstrates the lowest percentage of variation of E and H values, to reduce the strain levels in between layers. Also, when the E and H values of the SG coatings are compared to those of the M75/YSZ25 coatings, they exhibit smaller mismatch than M_50FG/ M75/YSZ25 coatings. Therefore, the M_30SD and M_SG mullite coating do seem to be better candidates as bond coats for the type of system when using the M75/YSZ25 coating as transitional layer.

A graphic representation of the evolution of elastic modulus and hardness with time interval of the thermal treatment is given in **Fig.7 (a)** and **(b)**. An increase of the E and H values for the mullite coatings produced from the fused and crushed M_SG and spray-dried M_30SD powders after the high temperature exposure is observed. This is the typical behaviour expected for ceramic materials, which is caused by sintering effects.

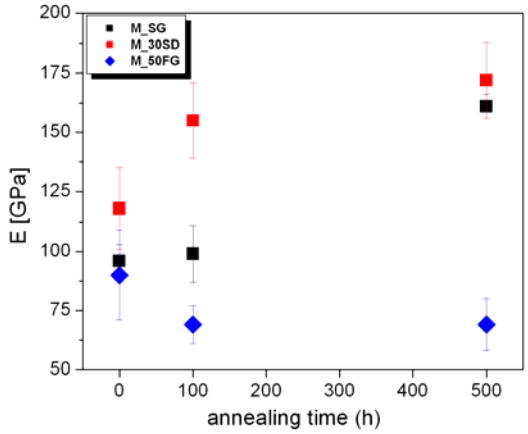

(a)

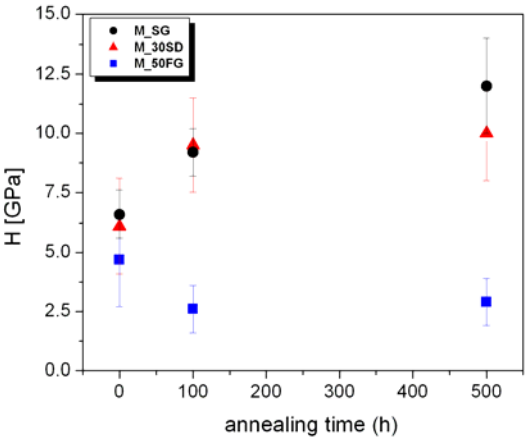

(b)

Fig. 7. (a) E and **(b)** H of thermally treated mullite coatings for time intervals up to 500 h

However, for the mullite coating produced from the freeze-granulated M_50FG powder, no increase of E and H values was noticed. This result is somewhat unexpected and up to this moment there are no clear explanations for that. When the overall as-sprayed and thermally treated microstructures of the mullite M_50FG coating are compared via SEM (not shown here), there are no signs of densification related to sintering. The M_50FG coating is highly porous, exhibiting a series of semi-molten particles embedded in the coating microstructure, which can be inferred due to its low E and H values. Therefore, due to the high porosity levels, it is speculated that the temperature of 1300^{o}C did not produce enough energy to cause the atomic diffusion necessary for sintering. Further experimental investigations will have to be performed to better understand this unexpected behaviour.

4 Conclusions

Fully crystalline mullite and YSZ-compositionally graded mullite coatings have been produced via thermal APS under controlled deposition conditions. The elastic modulus and hardness of the coatings have been investigated via instrumented indentation testing and an analysis of the values obtained for a 500 mN indentation load has been pursued. It was found via systematic measurements that both E and H values of the as-sprayed coatings are highly dependent on the morphology of the starting powders. As expected, a thermal treatment generally induced and increase of E and H values of the coatings produced from fused and crushed and spray-dried powders. However, the coating produced from the freeze granulated powder did not follow this general trend. It is speculated that its high porosity levels of the coating are creating a strong barrier against sintering and densification effects. It was identified a better match between the E and H values of the bond coat and subsequent layers obtained from powders having similar morphologies and size distribution (e.g. M_30SD/M_YSZ75/25vol%. Work is in progress to asses the E and H mismatch in YSZ compositionally graded tri-layers and ultimately in architectures having a 100% YSZ top coat.

5 Acknowledgments

The NRC team of authors acknowledges valuable technical support from its Surface Technology Group members for samples production, metallographic preparation and SEM analysis. This work has been supported by NRC-CSIC program (project 2007CA003)

6 Literature

[1] Lee, K.N., Current Status of Environmental Barrier Coatings for Si-Based Ceramics, Surf. Coat. Technol., 133-134 (2000), pp. 1/7.

[2] Schneider, H., Schreuer, J., and Hildmann, B., Structure and properties of mullite:A review, J. Eur. Ceram. Soc. 28 (2008), pp. 329/344.

[3] Jacobson, N.S., Corrosion of Silicon-Based Ceramics in Combustion Environments, J. Am. Ceram. Soc. 76, (1993), pp.3/28.

[4] Jacobson, N.S., Fox, D.S., Smialek, J.S., Opila, E.J., Dellacorte, C., and Lee, K.N., Performance of ceramics in severe environments, ASM Handbook, vol. 13B Corrosion Materials, pp. 565.

[5] Schulz, U. , Peters, M., Bachb, Fr.-W., and Tegeder, G. , Graded coatings for thermal, wear and corrosion barriers, Mat. Sci. and Eng. A 362 (2003), pp. 61/80.

[6] Murray, T.W. , Balogun, O., Steen, T.L. , Basu, S.N., and Sarin, V.K. , Inspection of compositionally graded mullite coatings using laser based ultrasonics, International Journal of Refractory Metals & Hard Materials 23 (2005), pp. 322/329.

[7] Cano, C., Garcia, E., Fernandes, A.L., Osendi, M.I., and Miranzo, P., Mullite/ZrO_2 coatings produced by flame spraying, J. Eur. Ceram. Soc. 28 (2008), pp. 2191/2197.

[8] Garcia, E., Mesquita-Guimarães, J. , Miranzo, P., and Osendi, M. I. , Procedure for obtaining ceramic feedstock for thermal spraying applications, Patent 2009, ICV-CSIC.

[9] Lima, R.S., Wang, Y., and Moreau, C., Patent 2008, NRC-IMI.

[10] Oliver, W.C., and Pharr, G.M., An improved technique for determining hardness and elastic modulus using load and displacement sensing indentation experiments, J. of Mat. Research, 7, issue 6 (1992), pp. 1564/1583.

[11] Garcia, E., Mesquita-Guimarães, J., Miranzo P., and Osendi, M. I., Cojocaru, C.V., Wang, Y., Moreau C., and Lima, R.S., Phase composition and microstructural responses of crystalline mullite/YSZ coating under water vapor environments ITSC2010, Singapore, proceedings.

[12] Elmustafaa, A.A., Stone, and D.S., Nanoindentation and the indentation size efect:Kinetics of deformation and strain gradient plasticity, Journal of the Mechanics and Physics of Solids, 51 (2003), pp. 357 /381.

[13] Jang, B.-K., Influence of low indentation load on Young's modulus and hardness of 4mol% Y_2O_3-Zr_2 by nanoindentation, J. of Alloys and Comp. 426 (2006), pp. 312/315.

[14] Cojocaru, C.V., Kruger, S., Moreau, C., and Lima, R.S., Mechanical Properties and Behaviour of BSAS/mullite-based Environmental Barrier Coatings Exposed to High Temperature in Water Vapour Environment, ITSC2010, Singapore, proceedings.